HEALTH AND MEDICINE

The obesity-induced adipokine sST2 exacerbates adipose T_{reg} and ILC2 depletion and promotes insulin resistance

Xu-Yun Zhao[1,2,3]*, Linkang Zhou[1], Zhimin Chen[1], Yewei Ji[4], Xiaoling Peng[1], Ling Qi[4], Siming Li[1], Jiandie D. Lin[1]*

Depletion of fat-resident regulatory T cells (T_{regs}) and group 2 innate lymphoid cells (ILC2s) has been causally linked to obesity-associated insulin resistance. However, the molecular nature of the pathogenic signals suppress adipose T_{regs} and ILC2s in obesity remains unknown. Here, we identified the soluble isoform of interleukin (IL)–33 receptor ST2 (sST2) as an obesity-induced adipokine that attenuates IL-33 signaling and disrupts T_{reg}/ILC2 homeostasis in adipose tissue, thereby exacerbates obesity-associated insulin resistance in mice. We demonstrated sST2 is a target of TNFα signaling in adipocytes that is countered by Zbtb7b. Fat-specific ablation of Zbtb7b augments adipose sST2 gene expression, leading to diminished fat-resident T_{regs}/ILC2s, more pronounced adipose tissue inflammation and fibrosis, and impaired glucose homeostasis in mice. Mechanistically, Zbtb7b suppresses NF-κB activation in response to TNFα through destabilizing IκBα. These findings uncover an adipokine-immune signaling pathway that is engaged in obesity to drive the pathological changes of the immunometabolic landscape.

INTRODUCTION

White adipose tissue (WAT) functions as an energy reservoir and regulates systemic metabolic physiology by releasing hormones, cytokines, and bioactive metabolites (*1*). In response to chronic overnutrition, white fat undergoes marked expansion to accommodate the increasing demand for energy storage, leading to excess adiposity and obesity (*2*). Adipose tissue expansion is accompanied by remodeling of the stromal and vascular compartments and profound changes in its immunological milieu (*3*, *4*). In obesity, adipocytes release an array of proinflammatory cytokines and chemokines, including tumor necrosis factor–α (TNFα), interleukin 6 (IL-6), and C-C motif chemokine ligand 2 (CCL2), leading to increased recruitment of proinflammatory immune cells, including macrophages (*5*–*7*), T helper 1 (T_H1) or T_H17 lymphocytes (*8*), and mast cells (*9*, *10*). This proinflammatory polarization of immune signaling is accompanied by depletion of resident regulatory T cells (T_{regs}) and group 2 innate lymphoid cells (ILC2s) in fat depot, contributing to obesity-associated adipose dysfunction and insulin resistance (*11*–*14*). Despite this, the mechanisms underlying the disruptions of adipose tissue T_{reg} and ILC2 homeostasis during obesity remain poorly understood.

IL-33 is a member of the IL-1 family of nuclear cytokines that is abundantly expressed in endothelial cells, epithelial cells, and fibroblast-like cells (*15*, *16*). It is released upon cell injury or tissue damage and functions as an alarmin to counter excess inflammatory response by targeting resident immune cells in the tissue that express its receptor suppression of tumorigenicity 2 (ST2; encoded by *Il1rl1*) (*13*, *17*). The IL-33/ST2 signaling pathway exerts diverse biological effects on T_{regs} (*18*, *19*), T_H2 lymphocytes (*20*, *21*), mast cells (*22*, *23*), and ILC2s (*13*, *24*) and has been implicated in the pathogenesis of allergic, fibrotic, infectious, and chronic inflammatory diseases (*17*, *25*). Two alternatively spliced isoforms of ST2 have been identified to generate full-length receptor (ST2L) mediating IL-33 signaling and soluble ST2 (sST2). The latter contains the extracellular domain responsible for IL-33 binding but lacks the transmembrane and intracellular domain. Hence, sST2 functions as a decoy receptor capable of IL-33 binding, thereby attenuating IL-33 signaling through its receptor ST2L (*26*). Recent studies demonstrated that mice lacking ST2 or IL-33 exhibited increased adiposity and worsened metabolic profiles following high-fat diet (HFD) feeding (*27*, *28*). IL-33 treatment was sufficient to trigger the expansion of a unique group of $Foxp3^+ST2^+$ T_{regs}, attenuate adipose tissue inflammation, and ameliorate insulin resistance (*29*, *30*). In this study, we uncovered sST2 as an obesity-induced adipokine that contributes to T_{reg} and ILC2 dysregulation and insulin resistance. Our work demonstrates that Zbtb7b serves as a checkpoint to restrict TNFα-induced expression and secretion of sST2 by adipocytes.

RESULTS

Obesity-associated reduction of adipose T_{regs} is linked to elevated expression and secretion of sST2

Depletion of adipose tissue resident T_{regs} and ILC2s is a prominent feature of immunometabolic dysregulations in obesity (*11*–*14*). Accordingly, mRNA expression of the T_{reg} marker Foxp3 in epididymal WAT (eWAT) was inversely correlated with the degree of obesity in

[1]Life Sciences Institute and Department of Cell and Developmental Biology, University of Michigan Medical Center, Ann Arbor, MI 48109, USA. [2]Department of Biochemistry and Molecular Cell Biology, Shanghai Key Laboratory for Tumor Microenvironment and Inflammation, Key Laboratory of Cell Differentiation and Apoptosis of National Ministry of Education, Shanghai Jiao Tong University School of Medicine, Shanghai, China. [3]Department of Cardiology, Shanghai Chest Hospital, Shanghai Jiao Tong University, Shanghai, China. [4]Department of Molecular and Integrative Physiology, University of Michigan Medical Center, Ann Arbor, MI 48109, USA.
*Corresponding author. Email: jdlin@umich.edu (J.D.L.); xuyunzhao@shsmu.edu.cn (X.-Y.Z.)

a cohort of HFD-fed mice (Fig. 1A) (*31*). Unexpectedly, IL-33 expression exhibited an opposite pattern of regulation, and its mRNA and protein levels were elevated in eWAT from obese mice (Fig. 1A and fig. S1, A to B). Two alternatively spliced isoforms of *Il1rl1* have been identified to generate full-length ST2L for IL-33 signaling and sST2 (Fig. 1B). The latter functions as a decoy receptor that diminishes IL-33 signaling. Gene expression analysis indicated that, while ST2L mRNA levels in brown adipose tissue (BAT), eWAT, and inguinal WAT (iWAT) were comparable between obese and lean mice, mRNA expression of sST2 was markedly elevated in adipose tissue from HFD-fed mice. Moderately increased expression of sST2 was also observed in the brain, lung, and spleen from obese mice (Fig. 1C). To determine the cellular sources of sST2 expression, we separated cells of the stromal vascular fraction (SVF) and adipocytes from lean and HFD-fed obese mouse eWAT. Quantitative polymerase chain reaction (qPCR) analysis revealed that sST2 mRNA expression was strongly induced in adipocytes from HFD-fed mice compared to control (Fig. 1D and fig. S1C).

We next measured sST2 secretion by eWAT explants using enzyme-linked immunosorbent assay (ELISA). Consistent with gene expression results, the concentration of sST2 in conditioned media was significantly higher in eWAT explants obtained from obese mice compared to lean control (Fig. 1E). It has been established that IL-33 signaling regulates adipose T_{regs} during obesity (*29*). To test whether sST2 attenuates IL-33 signaling and diminishes its function, we performed treatments in eWAT explant culture and examined the expression of genes responsive to IL-33 stimulation. While IL-33 treatment increased the expression of genes enriched in T_{regs} (*Foxp3*, *Klrg1*, and *Il2ra*) and ILC2s (*Il5*), this stimulatory effect was nearly abolished in the presence of recombinant sST2 (Fig. 1F). Together, these results demonstrated that obesity is linked to induction of sST2 expression and secretion by adipocytes. In addition, elevated sST2

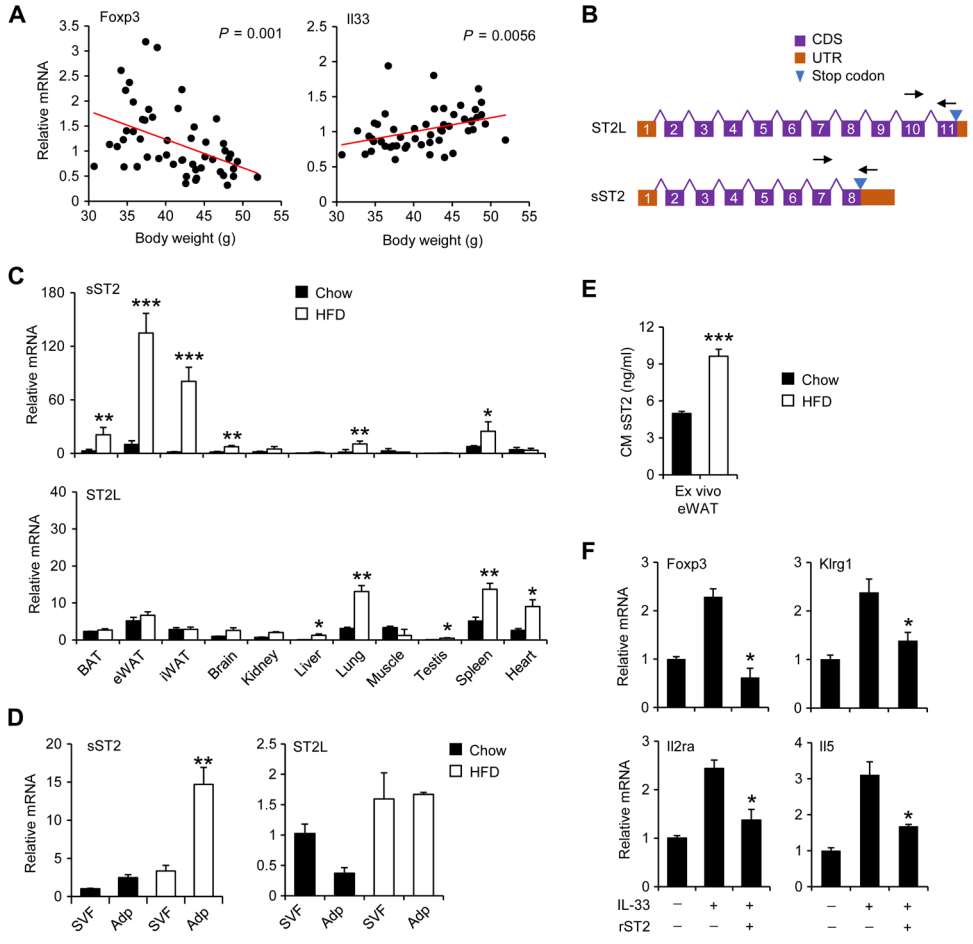

Fig. 1. Obesity-associated reduction of adipose T_{regs} is linked to elevated expression and secretion of sST2. (**A**) Correlation between eWAT Foxp3 and IL-33 mRNA levels and body weight in a cohort of C57BL/6J mice fed HFD for 8 weeks. (**B**) Schematic diagrams of the ST2 isoforms. Arrows indicate the location of isoform-specific qPCR primers. (**C**) qPCR analysis of sST2 and ST2L expression in a panel of tissues from mice fed chow (filled, $n = 4$) and HFD (open, $n = 4$). Data in (C) represent means ± SEM. $^*P < 0.05$, $^{**}P < 0.01$, $^{***}P < 0.001$, lean versus obese, two-tailed unpaired Student's *t* test. (**D**) qPCR analysis of gene expression in stromal vascular fraction (SVF) and adipocytes (Adp) isolated from eWAT from lean (filled, $n = 3$) and HFD-fed (open, $n = 3$) mice. Data represent means ± SEM. $^{**}P < 0.01$, SVF versus Adp, two-way ANOVA. (**E**) Concentrations of sST2 in conditioned media (CM) from eWAT explant culture from chow- and HFD-fed mice ($n = 3$). (**F**) qPCR analysis of gene expression in eWAT explants from HFD-fed mice ($n = 3$) treated with IL-33 (10 ng/ml) without or with recombinant sST2 (100 ng/ml). Data in (E) and (F) represent means ± SEM. $^*P < 0.05$, $^{***}P < 0.001$, chow versus HFD (E) and rST2 + IL-33 versus IL-33 (F), two-tailed unpaired Student's *t* test. Data in (C) to (F) are representative of three independent experiments.

may diminish local IL-33 signaling and contribute to reduced adipose tissue T_{regs} during obesity.

AAV-mediated elevation of sST2 exacerbates HFD-induced insulin resistance

To determine the role of sST2 in the regulation of adipose T_{regs} and metabolic physiology in obesity, we generated a recombinant AAV vector expressing sST2 under the control of CAG promoter (AAV-sST2). Wild-type (WT) mice were transduced with AAV–green fluorescent protein (GFP) or AAV-sST2 via tail vein injection and subjected to HFD feeding for 10 weeks. As expected, we observed robust sST2 overexpression in the liver, but not eWAT, BAT, and lung, and markedly elevated plasma sST2 levels (1.5 to 2 μg/ml) in mice transduced with AAV-sST2 (fig. S2, A and B). AAV-mediated overexpression of sST2 did not appear to affect mRNA expression of the long isoform ST2L in mouse tissues. Both groups of mice exhibited comparable body and tissue weight following HFD feeding (Fig. 2A and fig. S2C). While blood glucose concentrations were similar in two groups under fed condition, plasma insulin levels were elevated in mice transduced with AAV-sST2 (Fig. 2B). Under fasting condition, blood glucose and plasma insulin concentrations were slightly but significantly elevated in the AAV-sST2 group, suggesting that sST2 overexpression impairs glucose homeostasis in obesity. In support of this, glucose tolerance test (GTT) and insulin tolerance test (ITT) indicated that mice transduced with AAV-sST2 exhibited worsened glucose intolerance and insulin resistance (Fig. 2C).

Histological studies revealed that mice transduced with AAV-sST2 exhibited more abundant crown-like structures (CLS), a characteristic of adipose tissue inflammation and dysfunction, and more pronounced fibrosis, as revealed by Sirius red staining of collagen (Fig. 2D). qPCR analysis indicated that mRNA expression of genes enriched in T_{regs} (*Foxp3*, *Ctla4*, *Klrg1*, *Cd5*, *Icos*, and *Gata3*) in

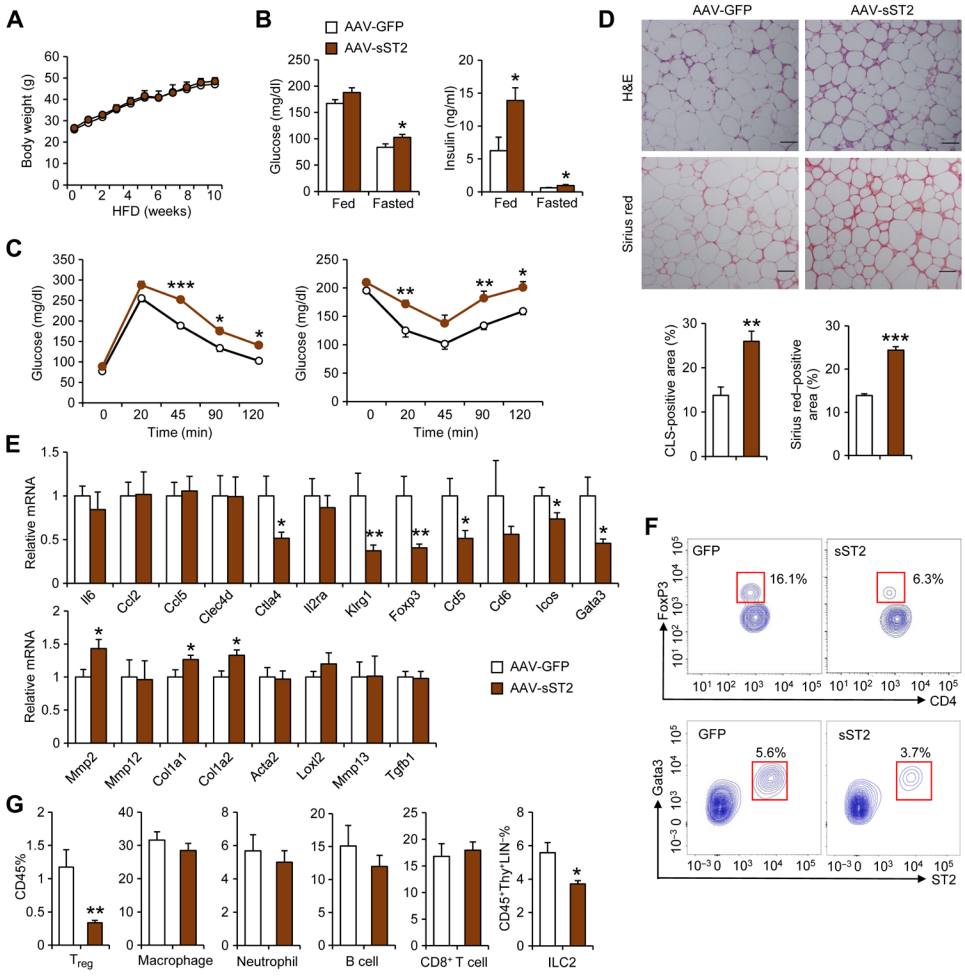

Fig. 2. Overexpression of sST2 exacerbates HFD-induced insulin resistance. (**A**) Body weight of mice transduced with AAV-GFP (open, $n = 5$) and AAV-sST2 (filled, $n = 6$) fed HFD for 10 weeks. Data represent means ± SEM, two-way ANOVA with multiple comparisons. (**B**) Blood glucose and plasma insulin concentrations. Data represent means ± SEM. $^*P < 0.05$, GFP versus sST2, two-tailed unpaired Student's *t* test. (**C**) GTT (left) and ITT (right) in mice transduced with AAV-GFP (open, $n = 6$) or AAV-sST2 (filled, $n = 7$) after 9 and 11 weeks of HFD feeding, respectively. Data represent means ± SEM. $^*P < 0.05$, $^{**}P < 0.01$, $^{***}P < 0.001$, GFP versus sST2, two-way ANOVA with multiple comparisons. Data in (A) to (C) are representative of three independent experiments. (**D**) Hematoxylin and eosin (H&E) and Sirius red staining of eWAT sections (top) and quantitation of CLS- and fibrosis-positive area (bottom). (**E**) qPCR analysis of eWAT gene expression. (**F**) Representative gating for resident T_{regs} and ILC2s in eWAT from transduced mice. (**G**) Percentage of immune cells in $CD45^+$ SVF cells. Data in (E) and (G) represent means ± SEM. $^*P < 0.05$, $^{**}P < 0.01$, GFP versus sST2, two-tailed unpaired Student's *t* test. Data in (D) to (G) are representative of three independent experiments. Scale bar = 100 μm.

eWAT was significantly decreased in mice overexpressing sST2 compared to control (Fig. 2E). In contrast, mRNA expression of extracellular matrix–related genes (Mmp2, Col1a1, and Col1a2) was elevated. Consistently, flow cytometry analysis revealed that $Foxp3^+$ $CD4^+$ adipose-resident T_{regs}, a major cell type regulated by IL-33 signaling, were reduced by approximately 60% in mice transduced with AAV-sST2 (Fig. 2, F and G). Similarly, $GATA3^+ST2^+$ ILC2s were also greatly diminished in response to sST2 overexpression. Other immune cell populations including macrophage, neutrophil, $CD8^+$ T cells, and B cells remained largely unaltered. Liver histology, fat content, and hepatic gene expression were largely unaltered by sST2 overexpression (fig. S2, D and E). Previous studies have demonstrated that activation of the IL-33/ST2 signaling pathway promotes thermogenic fat development (*32*, *33*). However, we did not observe obvious changes in BAT histology and thermogenic gene expression in HFD-fed mice in response to sST2 (fig. S2, F and G). These observations demonstrate that systemic elevation of sST2 impairs the maintenance of adipose tissue T_{regs} and ILC2s and disrupts glucose homeostasis in mice.

Adipocyte sST2 expression and secretion is stimulated by TNFα, which is antagonized by Zbtb7b expression

We next examined the nature of upstream signals that trigger the induction of sST2 expression in adipocytes. In a cohort of HFD-fed obese mice, mRNA expression of sST2 in eWAT exhibited strong correlation with obesity and adipose Ccl2 expression (Fig. 3A). To explore the potential role of proinflammatory cytokines in stimulating sST2 expression in obesity, we treated differentiated C3H10T1/2

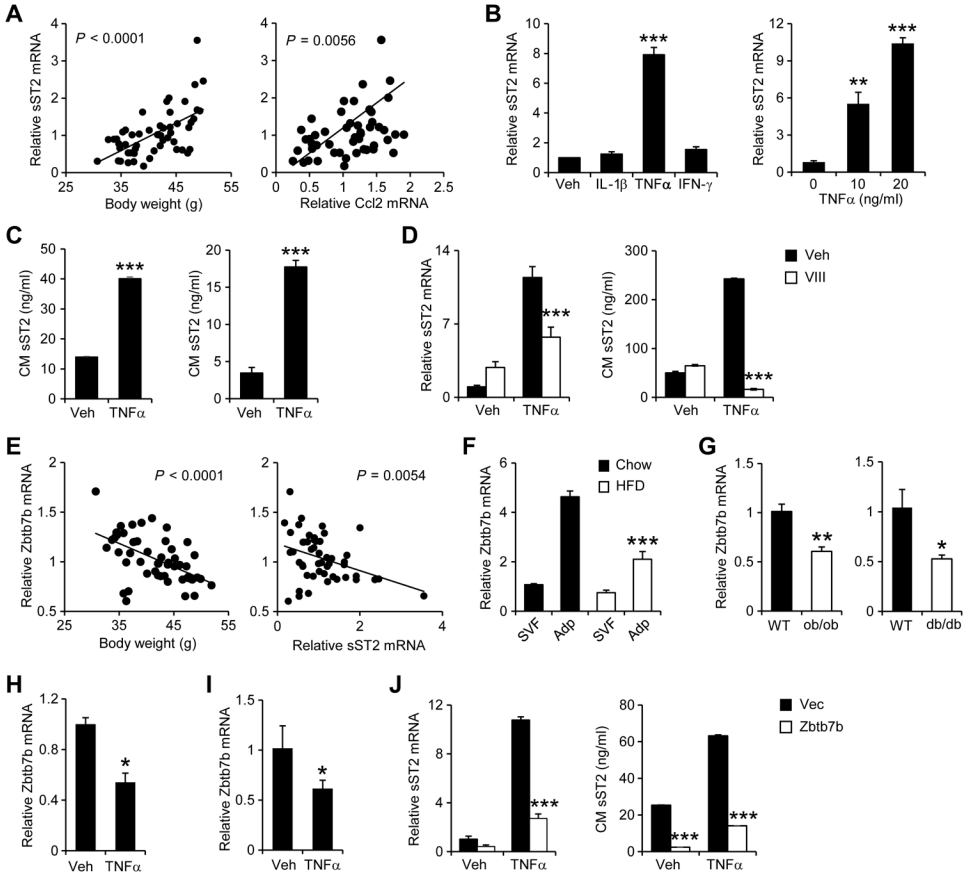

Fig. 3. Adipocyte sST2 expression and secretion are stimulated by TNFα, which is antagonized by Zbtb7b. (**A**) Correlation between eWAT sST2 gene expression and body weight (left) and Ccl2 expression (right). (**B**) qPCR analysis of sST2 mRNA expression in differentiated C3H10T1/2 adipocytes treated with vehicle (Veh), IL-1β (10 ng/ml), TNFα (10 ng/ml), or IFN-γ (10 ng/ml) for 24 hours (left) or indicated doses of TNFα (right). Data represent means ± SD ($n = 3$). $^{**}P < 0.01$, $^{***}P < 0.001$, versus Veh, one-way ANOVA. (**C**) The concentrations of sST2 in CM from C3H10T1/2 adipocytes (left) or eWAT explant culture (right) treated with Veh or TNFα (10 ng/ml) for 24 hours. Data represent means ± SD ($n = 3$). $^{***}P < 0.001$, Veh versus TNFα, two-tailed unpaired Student's *t* test. (**D**) sST2 mRNA expression (left) and concentrations (right) in adipocytes treated with TNFα (10 ng/ml) with or without NF-κB inhibitor VIII (VIII; 4 μM) for 24 hours. Data represent means ± SD ($n = 3$). $^{***}P < 0.001$, Veh versus VIII, two-way ANOVA. Data in (B) to (D) are representative of three independent experiments. (**E**) Correlation between eWAT mRNA expression of Zbtb7b and bodyweight (left) and sST2 (right) in HFD-fed mice. (**F**) qPCR analysis of Zbtb7b expression in SVF and adipocytes isolated from chow-fed (filled, $n = 3$) or HFD-fed (open, $n = 3$) mouse eWAT. Data represent means ± SEM. $^{***}P < 0.001$, SVF versus Adp, two-way ANOVA. (**G**) qPCR analysis of Zbtb7b expression in eWAT from WT (filled, $n = 5$) and ob/ob (open, $n = 3$) or WT (filled, $n = 4$) and db/db (open, $n = 4$) mice. Data represent means ± SEM. $^{*}P < 0.05$, $^{**}P < 0.01$, lean versus obese, two-tailed unpaired Student's *t* test. (**H** and **I**) qPCR analysis of Zbtb7b expression in differentiated C3H10T1/2 adipocytes (H) and explant fat culture (I) treated with 10 ng/ml TNFα for 24 hours. Data in (H) and (I) represent means ± SEM. $^{*}P < 0.05$, Veh versus TNFα, two-tailed unpaired Student's *t* test. (**J**) sST2 mRNA expression (left) and concentrations in CM (right) from C3H10T1/2 adipocytes expressing vector (Vec) or Zbtb7b following treatment with TNFα (10 ng/ml) for 24 hours. Data represent means ± SD ($n = 3$). $^{***}P < 0.001$, Vec versus Zbtb7b, two-way ANOVA. Data in (F) to (J) are representative of three independent experiments.

adipocytes with inflammatory cytokines including IL-1β, TNFα, and interferon-γ (IFN-γ). Among these cytokines, only TNFα treatment increased sST2 mRNA expression in a dose-dependent manner (Fig. 3B). TNFα treatment significantly increased sST2 secretion by cultured adipocytes and ex vivo eWAT explants (Fig. 3C). To determine whether nuclear factor κB (NF-κB) signaling triggered by TNFα is required for sST2 induction, we treated differentiated C3H10T1/2 adipocytes with TNFα in combination with compound VIII, a potent inhibitor of NF-κB. Compound VIII treatment significantly diminished the induction of sST2 expression and the secretion in response to TNFα (Fig. 3D). These results suggest that enhanced TNFα/NF-κB signaling may drive the induction of adipose sST2 expression and secretion during obesity.

We previously demonstrated that the transcription factor Zbtb7b promotes adipose thermogenesis and suppresses NF-κB signaling in white adipocytes (*34*, *35*). Zbtb7b mRNA expression was inversely correlated with adiposity and eWAT expression of sST2 in a cohort of HFD-fed WT mice (Fig. 3E). Cell fractionation studies indicated that Zbtb7b mRNA expression was diminished in adipocytes, but not SVF, isolated from eWAT from HFD-fed obese mice (Fig. 3F). Similarly, mRNA expression of Zbtb7b was significantly reduced in eWAT from ob/ob and db/db mice compared to WT control (Fig. 3G). TNFα treatment suppressed Zbtb7b expression in both differentiated C3H10T1/2 adipocytes and eWAT explants (Fig. 3, H and I). Because eWAT Zbtb7b and sST2 expression exhibited strong negative correlation, we next examined whether Zbtb7b may regulate sST2 expression in adipocytes. We transduced C3H10T1/2 preadipocytes with control vector or a recombinant retroviral vector expressing Zbtb7b, followed by adipogenic induction. As shown in Fig. 3J, Zbtb7b overexpression markedly attenuated the induction of sST2 mRNA expression and secretion in response to TNFα treatment. These results illustrate that Zbtb7b is a negative regulator of sST2 expression and secretion in adipocytes.

Adipose tissue–specific inactivation of Zbtb7b exacerbates insulin resistance and T_{reg} depletion during obesity

To address the role of Zbtb7b in adipose T_{reg} regulation and whole-body metabolism, we generated adipocyte-specific Zbtb7b knockout mice (ZAKO) by crossing Zbtb7b flox mice with adiponectin-Cre transgenic mice. Upon HFD feeding, flox/flox control (Flox) and ZAKO mice gained comparable body weight (fig. S3A). While adipose tissue/body weight ratio was similar between two genotypes, ZAKO mice had slightly larger liver compared to control (fig. S3B). Following HFD feeding, ZAKO mice exhibited higher blood glucose under ad lib and fasting conditions and elevated plasma insulin levels in the fed state, suggesting that inactivation of Zbtb7b in adipocytes impairs whole-body glucose homeostasis (Fig. 4A). In support of this, GTT and ITT experiments indicated that ZAKO mice developed more severe glucose intolerance and insulin resistance following HFD feeding (Fig. 4B). To directly assess insulin action in adipose tissue, we performed insulin injection and examined its downstream signaling pathway in eWAT from HFD-fed mice. As expected, insulin robustly stimulated phosphorylation of AKT, p70S6K, and S6 (Fig. 4C and fig. S4A). Insulin-stimulated phosphorylation of these proteins was greatly diminished in eWAT from ZAKO mice compared to control. Consistently, the effects of insulin to suppress lipolysis and ketogenesis were also attenuated, as revealed by elevated plasma concentrations of nonesterified fatty acids (NEFAs) and β-hydroxybutyrate in ZAKO mice following insulin injection (Fig. 4D). Histological staining revealed more abundant CLS and more severe fibrosis in ZAKO mouse eWAT following HFD feeding (Fig. 4E). Hepatic steatosis was also worsened in ZAKO mice (Fig. 4, E and F). These results demonstrate that inactivation of Zbtb7b in adipocytes exacerbates diet-induced metabolic disorders in mice.

As shown above, overexpression of Zbtb7b was sufficient to dampen TNFα-induced expression and secretion of sST2 by adipocytes (Fig. 3J). We next performed TNFα treatments in eWAT explant culture from chow-fed Flox and ZAKO mice. Gene expression analysis indicated that Zbtb7b inactivation strongly augmented the induction of sST2 expression in response to TNFα (Fig. 4G). Accordingly, sST2 secretion was significantly elevated in ZAKO eWAT explants compared to control. Increased secretion of sST2 was similarly observed in eWAT explants from HFD-fed ZAKO mice (Fig. 5A). As a result, plasma concentration of sST2 was also elevated in ZAKO mice following HFD feeding. We next examined the effects of Zbtb7b deficiency on adipose tissue T_{regs}/ILC2s. Flow cytometry analysis revealed that $Foxp3^+CD4^+$ fat-resident T_{regs} and $GATA3^+ST2^+$ ILC2 cells were significantly reduced in eWAT from HFD-fed ZAKO compared to control group (Fig. 5, B and C). In contrast, other immune cell populations including macrophage, neutrophil, $CD8^+$ T cell, and B cell were comparable between two groups. qPCR analysis of gene expression indicated that ZAKO mice displayed higher expression of extracellular matrix genes [matrix metalloproteinase 2 (*Mmp2*) and *Mmp12*] and fibrosis genes (*Col1a1* and *Loxl2*) and lower expression of genes enriched in T_{regs} (*Ctla4*, *Foxp3*, *Cd5*, *Cd6*, and *Icos*). mRNA expression of sST2 was significantly higher in ZAKO mouse eWAT than control (Fig. 5D). BAT histology and gene expression remained largely unaltered by Zbtb7b inactivation in HFD-fed mice (fig. S3, C and D). Although the sST2 level in the serum is slightly higher in the ZAKO mice, mRNA expression of T_{reg}- and ILC2-enriched genes was comparable in the spleen and lung (fig. S3E). As a decoy receptor for IL-33, increased local synthesis of sST2 is expected to attenuate IL-33 signaling and T_{reg} homeostasis in adipose tissue. To directly assess this, we performed IL-33 treatments in eWAT explant culture from Flox and ZAKO mice. As shown in Fig. 5E, the induction of IL-33–responsive genes, including *Foxp3*, *Il2ra*, *Klrg1*, *Gata3*, *Icos*, and *Il5*, were significantly attenuated by Zbtb7b deficiency. These results suggest that Zbtb7b serves as a checkpoint for sST2 secretion, IL-33 signaling, and resident T_{reg} homeostasis in adipose tissue.

Zbtb7b preserves IκBα in adipocyte in obesity by competing hnRNPU and β-TrCP interaction

NF-κB activation is governed by degradation of its inhibitory partner IκBα, which is mediated by the E3 ubiquitin ligase β-transducin repeat-containing protein (β-TrCP) (*36*). To explore the underlying mechanism through which Zbtb7b suppresses NF-κB signaling, we examined IκBα and β-TrCP protein expression in eWAT from HFD-fed Flox and ZAKO mice. Compared to control, eWAT from ZAKO mice displayed lower IκBα and higher β-TrCP protein expression (Fig. 6A and fig. S4B). To directly probe the effects of Zbtb7b on NF-κB signaling, we performed TNFα treatments in adipocytes differentiated from C3H10T1/2 preadipocytes transduced with vector or retroviral Zbtb7b. Overexpression of Zbtb7b decreased β-TrCP expression in differentiated adipocytes and attenuated IκBα degradation upon TNFα treatment, leading to reduced NF-κB p65 phosphorylation (Fig. 6B and fig. S4C). Previous studies have established that direct interaction between heterogeneous nuclear ribonucleoprotein U (hnRNPU) and β-TrCP is critical for β-TrCP

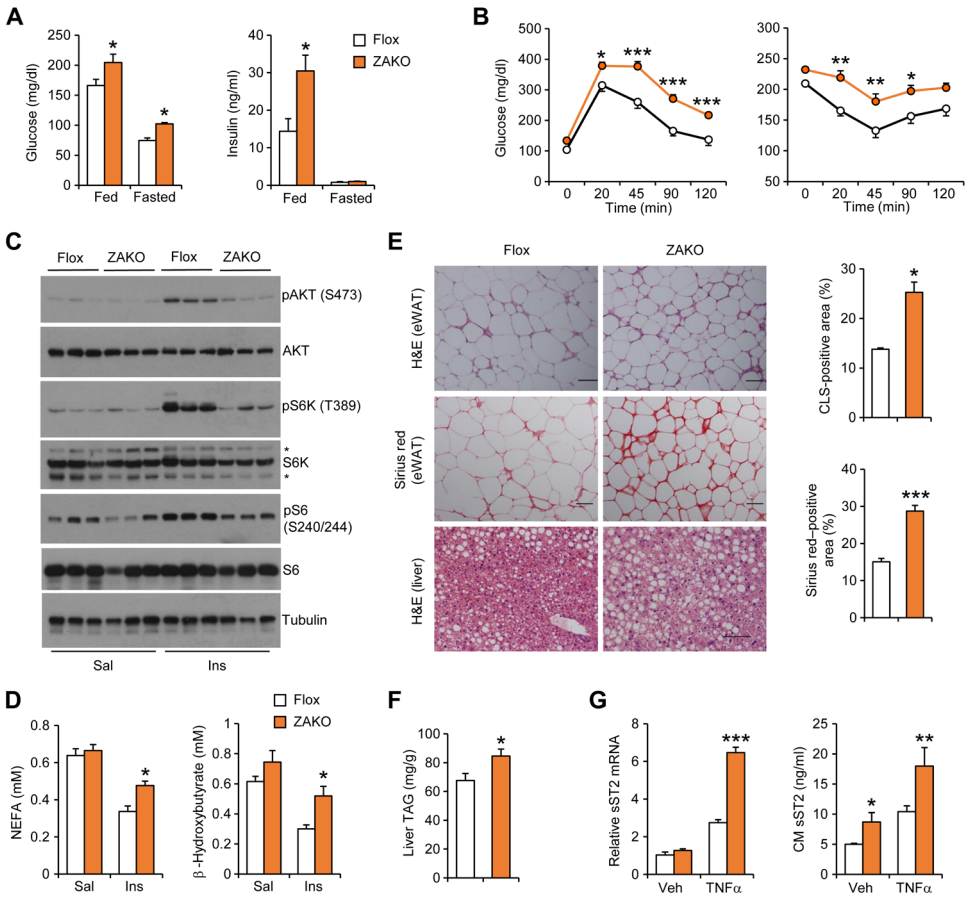

Fig. 4. Adipocyte-specific inactivation of Zbtb7b exacerbates insulin resistance. (**A**) Blood glucose and plasma insulin concentrations in HFD-fed control (Flox; $n = 12$) and ZAKO ($n = 9$) mice. Data represent means ± SEM. *$P < 0.05$, Flox versus ZAKO, two-tailed unpaired Student's t test. (**B**) GTT (left) and ITT (right) in Flox (open, $n = 12$) and ZAKO (filled, $n = 9$) mice fed HFD for 8 and 11 weeks, respectively. Data represent means ± SEM. *$P < 0.05$, **$P < 0.01$, ***$P < 0.001$, Flox versus ZAKO, two-way ANOVA with multiple comparisons. Data in (A) and (B) are representative of three independent experiments. (**C**) Immunoblots of eWAT lysates from Flox and ZAKO mice fed HFD for 13 weeks following intravenous injection of saline (Sal; Flox, open, $n = 7$; and ZAKO, filled, $n = 3$) and insulin (Ins; Flox, open, $n = 5$; and ZAKO, filled, $n = 5$) for 10 min. (**D**) Plasma nonesterified fatty acid (NEFA) and β-hydroxybutyrate concentrations in mice treated with saline or insulin. Data represent means ± SEM. *$P < 0.05$, Flox versus ZAKO, two-way ANOVA. (**E**) H&E and Sirius red staining of eWAT and liver sections in HFD-fed mice. Quantitation of CLS- and fibrosis-positive area is shown on the right. (**F**) Liver triglyceride (TAG) content. (**G**) mRNA expression (left) and secretion (right) of sST2 in explant fat culture from Flox and ZAKO mice treated with TNFα (10 ng/ml) for 24 hours. Data represent means ± SEM ($n = 4$). *$P < 0.05$, **$P < 0.01$, ***$P < 0.001$, Flox versus ZAKO, two-way ANOVA. Data in (E) to (G) are representative of three independent experiments. Scale bar = 100 μm.

protein stability (*37*). We recently identified that hnRNPU is an interaction partner for Zbtb7b in adipocyte (*34*). To determine whether Zbtb7b modulates hnRNPU/β-TrCP interaction, we transfected human embryonic kidney (HEK) 293 cells with expression constructs for hnRNPU and β-TrCP without or with Zbtb7b expression construct. Coimmunoprecipitation experiments showed that Zbtb7b weakened physical interaction between β-TrCP and hnRNPU (Fig. 6C). Furthermore, cycloheximide treatment experiment revealed that Zbtb7b reduced the half-life of β-TrCP, resulting in stabilization of IκBα (Fig. 6D and fig. S4D). These results support the mechanism that Zbtb7b inhibits NF-κB activity through competing hnRNPU/β-TrCP interaction and preserving IκBα protein levels in adipocytes.

DISCUSSION

Adipose tissue is an important source of endocrine hormones, such as leptin, adiponectin, and neuregulin 4, which act on the central nervous system and peripheral tissues to regulate diverse aspects of nutrient and energy metabolism (*38*–*40*). In addition, adipocytes release various cytokines and chemokines that promote the recruitment of immune cells and sustain chronic inflammation in adipose tissue during obesity. It has been established that depletion of adipose-resident T_{regs} and ILC2 is a prominent feature of the immunometabolic dysregulations in obesity and contributes to adipose tissue inflammation and insulin resistance (*11*–*14*). In this study, we identified sST2 as a obesity-associated adipokine that contributes to the disruption of adipose T_{reg} and ILC2 homeostasis and insulin sensitivity. We found that obesity triggers a strong induction of sST2 expression and secretion by adipocytes. AAV-mediated elevation of sST2 diminished adipose tissue T_{regs} and exacerbated HFD-induced adipose tissue inflammation and insulin resistance. At the mechanistic level, the transcription factor Zbtb7b attenuates TNFα-induced expression of sST2 through inhibiting NF-κB signaling. These findings establish sST2 as an obesity-linked

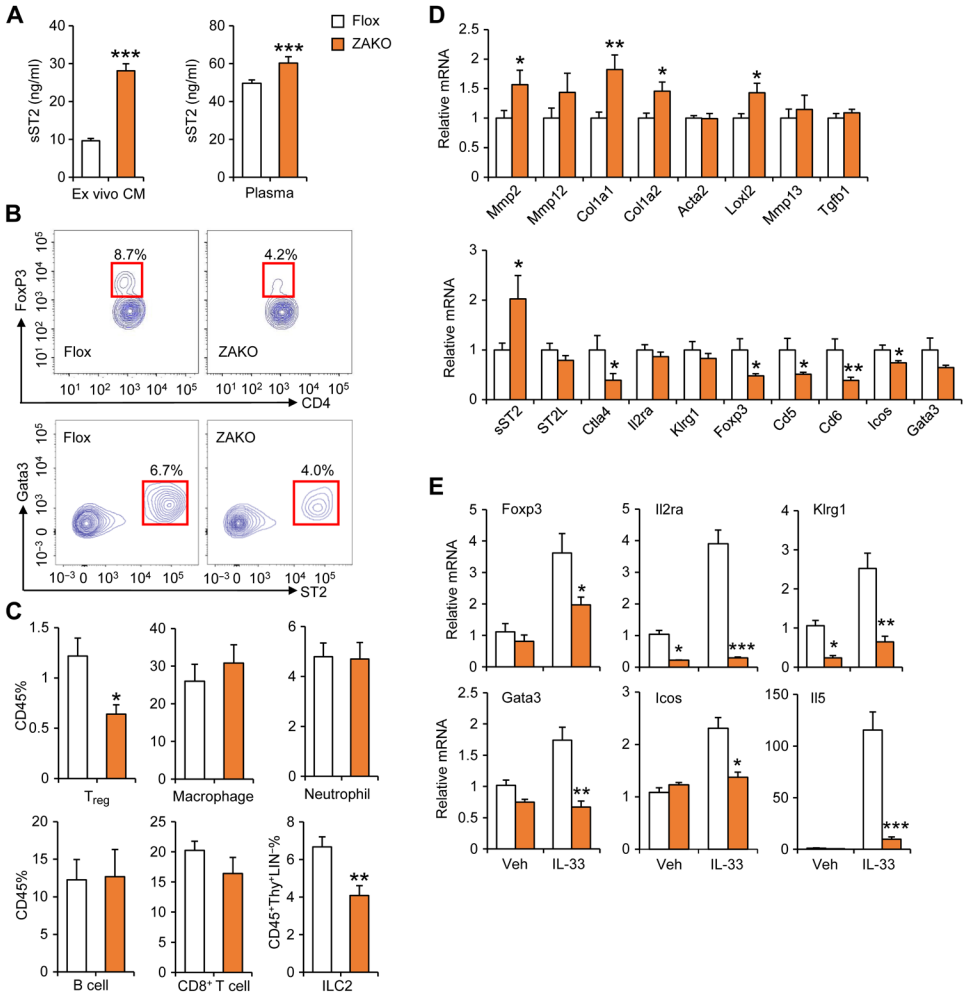

Fig. 5. Adipocyte-specific inactivation of Zbtb7b diminishes fat-resident T_{regs} and ILC2s. (**A**) sST2 concentration in CM from explant fat culture and plasma of HFD-fed Flox ($n = 12$) and ZAKO ($n = 9$) mice. (**B**) Representative gating for fat-resident T_{reg} and ILC2 cells from Flox and ZAKO mice. (**C**) Percentage of immune cells in $CD45^+$ SVF cells from HFD-fed Flox and ZAKO mice. (**D**) qPCR analysis of eWAT gene expression from Flox and ZAKO mice. Data in (A), (C), and (D) represent means ± SEM. $^*P < 0.05$, $^{**}P < 0.01$, $^{***}P < 0.001$; Flox versus ZAKO, two-tailed unpaired Student's *t* test. (**E**) qPCR analysis of gene expression in explant fat culture from HFD-fed Flox and ZAKO mice treated with IL-33 (40 ng/ml) for 24 hours. Data represent means ± SEM ($n = 6$). $^*P < 0.05$, $^{**}P < 0.01$, $^{***}P < 0.001$, Flox versus ZAKO, two-way ANOVA. Data in (A) to (E) are representative of three independent experiments.

adipokine that attenuates IL-33 signaling and exacerbates insulin resistance (Fig. 6E).

IL-33 derived from stromal cells has been shown to support the maintenance of resident T_{regs} and ILC2s in adipose tissue. However, adipose IL-33 expression was elevated in obesity, suggesting that a distinct mechanism may underlie obesity-associated disruption of T_{reg}/ILC2 homeostasis. Several lines of evidence support the notion that aberrant sST2 release by adipocytes may be a pathogenic factor here. First, sST2 expression in adipose tissue is highly correlated with adiposity and adipose tissue inflammatory gene expression. Recombinant sST2 blocks IL-33–induced expression of T_{reg} and ILC2 enriched genes in explant fat culture. AAV-mediated overexpression of sST2 further exacerbated obesity-associated depletion of T_{regs} and ILC2s in adipose tissue and worsened insulin resistance and glucose intolerance. These findings are consistent with previous studies that illustrated a critical role of IL-33/ST2L signaling in maintaining adipose T_{regs}/ILC2s and metabolic homeostasis. Mice deficient in IL-33 or ST2 developed greater adiposity and impaired glucose homeostasis (*27*, *41*).

Our previous studies have demonstrated that Zbtb7b is required for cold-induced thermogenesis and white fat browning in response to chronic cold exposure. However, we did not observe significant impairment of thermogenic gene expression in BAT by Zbtb7b deficiency in HFD-fed mice. These results suggest that, while Zbtb7b is critical for cold-induced thermogenesis, it appears to be dispensable for maintaining thermogenic capacity in diet-induced obesity. We did not observe significant differences in weight gain in Flox and ZAKO mice following HFD feeding. Hence, our data support a thermogenesis-independent mechanism in mediating the effects of Zbtb7b deficiency on adipose and systemic metabolism. In this study, we identified Zbtb7b as a transcriptional repressor for sST2 expression. Adipose tissue expression and secretion of sST2 were elevated in mice with adipocyte-specific deficiency of Zbtb7b. As a consequence, ZAKO mice exhibited several phenotypic features of

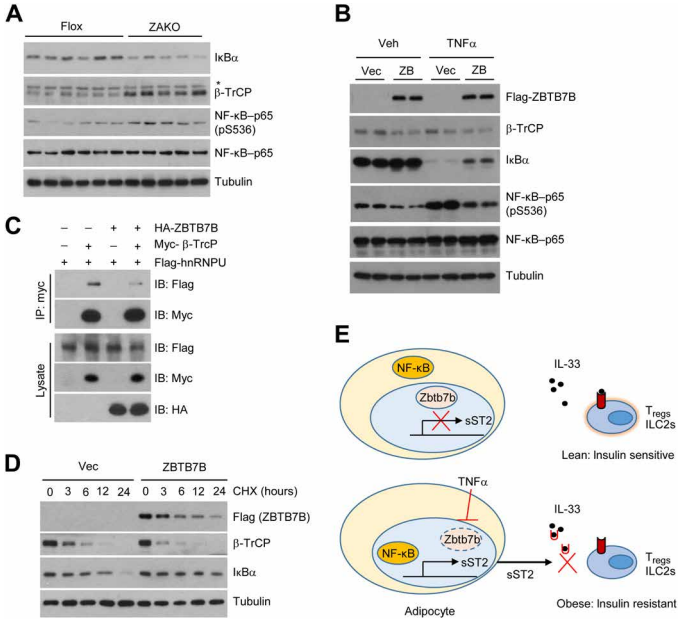

Fig. 6. Zbtb7b stabilizes IκBα by competing with β-TrCP for hnRNPU binding. (**A**) Immunoblots of total eWAT lysates from HFD-fed Flox and ZAKO mice. (**B**) Immunoblots of total lysates from C3H10T1/2 adipocytes expressing vector (vec) or Zbtb7b (ZB) treated with vehicle or TNFα (10 ng/ml) for 15 min. (**C**) Immunoblots of total lysates and α-Myc immunocomplexes from transiently transfected HEK293T cells. HA, hemagglutinin. (**D**) Immunoblots of total lysates from differentiated 10T1/2 adipocytes expressing Vec or Zbtb7b treated with cycloheximide (CHX; 100 μg/ml) for the indicated times. (**E**) A schematic model depicting the role of the Zbtb7b-sST2–IL-33 signaling pathway in the regulation of adipose tissue T_{reg}/ILC2 homeostasis and insulin sensitivity. Data in (A) to (D) are representative of three independent experiments.

impaired IL-33 signaling, including diminished adipose-resident T_{regs} and ILC2 cells that were accompanied by more severe HFD-induced metabolic disorders. Future work using cell type–specific sST2 knockout mice should clarify the significance of adipocyte-derived sST2 in obesity-associated T_{reg} depletion and insulin resistance.

Previous studies demonstrated that plasma sST2 level is significantly associated with metabolic characteristics of human diabetes (*42*); however, its cellular sources remain unknown. We found that obesity is linked to a drastic induction of sST2 in adipose tissue, which is primarily attributed to its increased expression in adipocytes. Among several proinflammatory cytokines, TNFα was identified as a potent inducer of sST2 gene expression in adipocytes. TNFα strongly stimulates the secretion of sST2 into conditioned media in cultured adipocytes and fat explants, indicating that local TNFα signaling plays an important role in modulating the secretion of other adipocyte-derived secreted factors during obesity. Hence, we previously demonstrated that the expression of Nrg4 in adipocytes is strongly inhibited by TNFα treatment. We identified Zbtb7b as a negative regulator of TNFα signaling and sST2 expression in adipocytes. In this case, Zbtb7b overexpression greatly diminished the induction of sST2 expression and secretion in response to TNFα, whereas fat explants from ZAKO mice exhibited augmented response to TNFα. While the exact mechanisms through which Zbtb7b suppresses sST2 expression remains to be established, it has become evident that Zbtb7b exerts an inhibitory effect on NF-κB activation. Together with the recent work on thermogenic gene regulation by Zbtb7b (*34*), our studies illustrate a scenario where metabolic and inflammatory gene programs are highly coordinated in adipocytes. The identification of sST2 as a deleterious adipokine reveals a potential target for interventions that restores immunometabolic homeostasis during obesity.

MATERIALS AND METHODS

Study design

The objective of this study was to explore the pathogenic mechanisms that drive obesity-associated disruption of immune signaling in adipose tissue. We used recombinant AAV vectors to overexpress sST2 in mice and generated a fat-specific Zbtb7b knockout mouse model (ZAKO) to dissect the role of the Zbtb7b-sST2 axis in adipose T_{reg}/ILC2 regulation and insulin resistance. We fed mice HFD to induce obesity and performed GTT and ITT and measured metabolic parameters to assess the contribution of sST2 and Zbtb7b deficiency to diet-induced insulin resistance and T_{reg}/ILC2 homeostasis. For sST2 overexpression studies, we randomly assigned C57BL/6J WT mice to receive tail vein injection of AAV-GFP or AAV-sST2. Age- and gender-matched Flox and ZAKO littermates were used for in vivo metabolic analyses and ex vivo adipose explant studies. The measurements were performed without the knowledge of mouse genotypes and treatments. All mouse experiments were independently replicated at least twice. The cell culture experiments were performed using triplicates and repeated at least three times. We did not exclude any data points or mice unless a technical issue or a human error had occurred.

Animals

All animal studies were performed according to procedures approved by the University Committee on Use and Care of Animals at the University of Michigan. WT C57BL/6J mice (JAX #000664) were purchased from the Jackson Laboratory. The Zbtb7b floxed mice were obtained from R. Bosselut from the National Cancer Institute. After crossing Zbtb7b floxed mice with adiponectin-Cre mice, exons 2 and 3 of Zbtb7b were deleted, as previously described (*43*). Mice were maintained in 12-hour light/12-hour dark cycles. Age-matched male WT mice were divided into two groups and fed regular rodent chow or HFD (D12492; Research Diets). HFD feeding was typically initiated at 3 months of age. For histology, tissues were dissected and fixed in 10% formalin overnight at 4°C and subjected to paraffin embedding and hematoxylin and eosin (H&E) staining. Sirius red staining was processed as previously described (*44*). Percentage of CLS and Sirius red staining positive area of the total area of view was quantified using ImageJ.

Adipose tissue explant culture

eWAT from WT and ZAKO mice was dissected and transferred to a culture dish with 10 ml of Dulbecco's modified Eagle's medium (DMEM). Fat pad was cut into approximately 4-mm pieces and washed sequentially with 10× volume phosphate-buffered saline and DMEM. Equal numbers of fat pieces were transferred into six-well plates with serum-free M199 media (1 nM insulin and 1 nM dexamethasone) and cultured for 24 hours before treatment. Following treatments, fat tissues were collected and processed for gene expression and immunoblotting analyses.

Immunoblotting analysis

Total cell lysates were prepared in a lysis buffer containing 50 mM tris-HCl (pH 7.8), 137 mM NaCl, 10 mM NaF, 1 mM EDTA, 1% Triton X-100, 10% glycerol, and the protease inhibitor cocktail (Roche) after three freeze/thaw cycles. Tissue lysates were prepared by homogenizing in a buffer containing 50 mM tris (pH 7.6), 130 mM NaCl, 5 mM NaF, 25 mM β-glycerophosphate, 1 mM sodium orthovanadate, 10% glycerol, 1% Triton X-100, 1 mM dithiothreitol, 1 mM phenylmethylsulfonyl fluoride, and the protease inhibitor cocktail. The antibodies used are as follows: rabbit anti-IκBα (4812), rabbit anti-β-TrCP (4394), phospho–NF-κB–p65 (S536 and 3033), and NF–κB–p65 (8242), which were purchased from Cell Signaling Technology. Mouse anti-Flag (F3165), mouse anti-myc (M5546), and mouse anti-tubulin (T6199) were purchased from Sigma-Aldrich. Rabbit anti–hemagglutinin (sc-805) was purchased from Santa Cruz Biotechnology.

Metabolic analyses

For GTT, mice were fasted overnight (16 hours) and injected intraperitoneally with a glucose solution at a dose of 1.0 g/kg body weight. For ITT, mice were prefasted for 4 hours and intraperitoneally injected with insulin at a dose of 1 U/kg body weight. Blood glucose concentrations were measured before and 20, 45, 90, and 120 min after glucose or insulin injection. Liver triglyceride was extracted and measured as previously described (*45*). Plasma insulin was measured using an ELISA kit (Crystal Chem).

Adipocyte differentiation

C3H10T1/2 cells expressing vector or Zbtb7b were maintained in DMEM supplemented with 10% fetal bovine serum (FBS). Confluent preadipocytes were subjected for differentiation by adding an induction medium containing 0.5 mM 3-isobutyl-1-methylxanthine, 125 μM indomethacin, 1 μM dexamethasone, 20 nM insulin, and 1 nM T3. Cells were switched to differentiation medium (DMEM, 10% FBS, 20 nM insulin, and 1 nM T3) after 2 days. TNFα and NF-κB inhibitor compound VIII treatments were performed in the fully differentiated adipocytes. Protein level of sST2 in the conditional medium and serum was measured using an ELISA kit (R&D Systems).

Gene expression analyses

Total RNA from differentiated adipocytes was extracted using the TRIzol method following manufacturer instructions. Total tissue RNA was isolated using the PureLink RNA isolation kit (Thermo Fisher Scientific). For reverse transcription qPCR, 2 μg of RNA was reverse-transcribed using M-MLV (Invitrogen), followed by qPCR using SYBR Green (Life Technologies). Relative mRNA expression was normalized to the expression of ribosomal protein 36B4. The qPCR primers used for gene expression are listed in table S1.

Flow cytometry analysis

Adipose tissue SVF isolation and flow cytometry were performed as previously described (*46*, *47*). Briefly, SVF was incubated in Fc Block (rat anti-mouse CD16/32; eBioscience) before staining with anti-CD45 (30-F11), CD3e (145-2C11), CD4 (GK1.5), CD8a (53-6.7), CD11c (N418), and CD64 (X54-5/7.1) (BD Pharmingen). For analysis of T_{regs}, the samples were fixed after surface staining, permeabilized with a FOXP3 Fix/Perm Buffer Set (421403; BioLegend), and stained with anti-FoxP3 (150D; BioLegend) antibody according to the manufacturer's protocol. For ILC2 cells, SVF was stained with anti-CD45 (30-F11), B220 (RA3-6B2), CD11b (M1/70), CD11c (N418), Gr-1 (RB6-8C5), CD3e (145-2C11), Thy1.2 (53-2.1) (BioLegend), ST2 (RMST2-2), and Gata3 (TWAJ) (eBioscience), as previously described (*11*). Samples were analyzed using a BD LSR cell analyzer at the Vision Research Core Facility at the University of Michigan Medical School. Data were analyzed using the FACSDiva v6.2 software (BD Biosciences) and Flowjo (Flowjo.com). Flow cytometry gating strategies for T_{regs}, B cells, macrophages, neutrophils, $CD8^+$ T cells, and ILC2s are shown in fig. S5.

Statistical analysis

Statistical analysis was performed using GraphPad Prism 7. Statistical differences were evaluated using two-tailed unpaired Student's *t* test for comparisons between two groups or analysis of variance (ANOVA) and appropriate post hoc analyses for comparisons of more than two groups. Two-way ANOVA with multiple comparisons was used for statistical analysis of body weight, GTT, and ITT. A *P* value of less than 0.05 ($^*P < 0.05$, $^{**}P < 0.01$, and $^{***}P < 0.001$) was considered statistically significant. Statistical methods and corresponding *P* values for data shown in each panel were included in the figure legends.

SUPPLEMENTARY MATERIALS

Supplementary material for this article is available at http://advances.sciencemag.org/cgi/content/full/6/20/eaay6191/DC1

View/request a protocol for this paper from *Bio-protocol*.

REFERENCES AND NOTES

1. J. H. Stern, J. M. Rutkowski, P. E. Scherer, Adiponectin, leptin, and fatty acids in the maintenance of metabolic homeostasis through adipose tissue crosstalk. *Cell Metab.* **23**, 770–784 (2016).
2. J. M. Rutkowski, J. H. Stern, P. E. Scherer, The cell biology of fat expansion. *J. Cell Biol.* **208**, 501–512 (2015).
3. G. Martinez-Santibañez, C. N. Lumeng, Macrophages and the regulation of adipose tissue remodeling. *Annu. Rev. Nutr.* **34**, 57–76 (2014).
4. Y. H. Lee, A. P. Petkova, J. G. Granneman, Identification of an adipogenic niche for adipose tissue remodeling and restoration. *Cell Metab.* **18**, 355–367 (2013).
5. C. N. Lumeng, J. L. Bodzin, A. R. Saltiel, Obesity induces a phenotypic switch in adipose tissue macrophage polarization. *J. Clin. Invest.* **117**, 175–184 (2007).
6. M. Kratz, B. R. Coats, K. B. Hisert, D. Hagman, V. Mutskov, E. Peris, K. Q. Schoenfelt, J. N. Kuzma, I. Larson, P. S. Billing, R. W. Landerholm, M. Crouthamel, D. Gozal, S. Hwang, P. K. Singh, L. Becker, Metabolic dysfunction drives a mechanistically distinct proinflammatory phenotype in adipose tissue macrophages. *Cell Metab.* **20**, 614–625 (2014).
7. H. Xu, G. T. Barnes, Q. Yang, G. Tan, D. Yang, C. J. Chou, J. Sole, A. Nichols, J. S. Ross, L. A. Tartaglia, H. Chen, Chronic inflammation in fat plays a crucial role in the development of obesity-related insulin resistance. *J. Clin. Invest.* **112**, 1821–1830 (2003).
8. S. Nishimura, I. Manabe, M. Nagasaki, K. Eto, H. Yamashita, M. Ohsugi, M. Otsu, K. Hara, K. Ueki, S. Sugiura, K. Yoshimura, T. Kadowaki, R. Nagai, $CD8^+$ effector T cells contribute to macrophage recruitment and adipose tissue inflammation in obesity. *Nat. Med.* **15**, 914–920 (2009).
9. M. M. Altintas, A. Azad, B. Nayer, G. Contreras, J. Zaias, C. Faul, J. Reiser, A. Nayer, Mast cells, macrophages, and crown-like structures distinguish subcutaneous from visceral fat in mice. *J. Lipid Res.* **52**, 480–488 (2011).
10. J. Liu, A. Divoux, J. Sun, J. Zhang, K. Clément, J. N. Glickman, G. K. Sukhova, P. J. Wolters, J. Du, C. Z. Gorgun, A. Doria, P. Libby, R. S. Blumberg, B. B. Kahn, G. S. Hotamisligil, G. P. Shi, Genetic deficiency and pharmacological stabilization of mast cells reduce diet-induced obesity and diabetes in mice. *Nat. Med.* **15**, 940–945 (2009).
11. X. Ding, Y. Luo, X. Zhang, H. Zheng, X. Yang, X. Yang, M. Liu, IL-33-driven ILC2/eosinophil axis in fat is induced by sympathetic tone and suppressed by obesity. *J. Endocrinol.* **231**, 35–48 (2016).
12. M. Feuerer, L. Herrero, D. Cipolletta, A. Naaz, J. Wong, A. Nayer, J. Lee, A. B. Goldfine, C. Benoist, S. Shoelson, D. Mathis, Lean, but not obese, fat is enriched for a unique population of regulatory T cells that affect metabolic parameters. *Nat. Med.* **15**, 930–939 (2009).

13. A. B. Molofsky, F. van Gool, H. E. Liang, S. J. van Dyken, J. C. Nussbaum, J. Lee, J. A. Bluestone, R. M. Locksley, Interleukin-33 and interferon-γ counter-regulate group 2 innate lymphoid cell activation during immune perturbation. *Immunity* **43**, 161–174 (2015).
14. S. Winer, Y. Chan, G. Paltser, D. Truong, H. Tsui, J. Bahrami, R. Dorfman, Y. Wang, J. Zielenski, F. Mastronardi, Y. Maezawa, D. J. Drucker, E. Engleman, D. Winer, H. M. Dosch, Normalization of obesity-associated insulin resistance through immunotherapy. *Nat. Med.* **15**, 921–929 (2009).
15. F. Roan, K. Obata-Ninomiya, S. F. Ziegler, Epithelial cell-derived cytokines: More than just signaling the alarm. *J. Clin. Invest.* **129**, 1441–1451 (2019).
16. M. Pichery, E. Mirey, P. Mercier, E. Lefrancais, A. Dujardin, N. Ortega, J. P. Girard, Endogenous IL-33 is highly expressed in mouse epithelial barrier tissues, lymphoid organs, brain, embryos, and inflamed tissues: In situ analysis using a novel *Il-33-LacZ* gene trap reporter strain. *J. Immunol.* **188**, 3488–3495 (2012).
17. F. Y. Liew, J. P. Girard, H. R. Turnquist, Interleukin-33 in health and disease. *Nat. Rev. Immunol.* **16**, 676–689 (2016).
18. D. Kolodin, N. van Panhuys, C. Li, A. M. Magnuson, D. Cipolletta, C. M. Miller, A. Wagers, R. N. Germain, C. Benoist, D. Mathis, Antigen- and cytokine-driven accumulation of regulatory T cells in visceral adipose tissue of lean mice. *Cell Metab.* **21**, 543–557 (2015).
19. C. Schiering, T. Krausgruber, A. Chomka, A. Fröhlich, K. Adelmann, E. A. Wohlfert, J. Pott, T. Griseri, J. Bollrath, A. N. Hegazy, O. J. Harrison, B. M. J. Owens, M. Löhning, Y. Belkaid, P. G. Fallon, F. Powrie, The alarmin IL-33 promotes regulatory T-cell function in the intestine. *Nature* **513**, 564–568 (2014).
20. J. Schmitz, A. Owyang, E. Oldham, Y. Song, E. Murphy, T. K. McClanahan, G. Zurawski, M. Moshrefi, J. Qin, X. Li, D. M. Gorman, J. F. Bazan, R. A. Kastelein, IL-33, an interleukin-1-like cytokine that signals via the IL-1 receptor-related protein ST2 and induces T helper type 2-associated cytokines. *Immunity* **23**, 479–490 (2005).
21. M. Komai-Koma, D. Xu, Y. Li, A. . N. . J. McKenzie, I. . B. McInnes, F. . Y. Liew, IL-33 is a chemoattractant for human Th2 cells. *Eur. J. Immunol.* **37**, 2779–2786 (2007).
22. H. Morita, K. Arae, H. Unno, K. Miyauchi, S. Toyama, A. Nambu, K. Oboki, T. Ohno, K. Motomura, A. Matsuda, S. Yamaguchi, S. Narushima, N. Kajiwara, M. Iikura, H. Suto, A. N. J. McKenzie, T. Takahashi, H. Karasuyama, K. Okumura, M. Azuma, K. Moro, C. A. Akdis, S. J. Galli, S. Koyasu, M. Kubo, K. Sudo, H. Saito, K. Matsumoto, S. Nakae, An interleukin-33-mast cell-interleukin-2 axis suppresses papain-induced allergic inflammation by promoting regulatory T cell numbers. *Immunity* **43**, 175–186 (2015).
23. D. Xu, H. R. Jiang, P. Kewin, Y. Li, R. Mu, A. R. Fraser, N. Pitman, M. Kurowska-Stolarska, A. N. J. McKenzie, I. B. McInnes, F. Y. Liew, IL-33 exacerbates antigen-induced arthritis by activating mast cells. *Proc. Natl. Acad. Sci. U.S.A.* **105**, 10913–10918 (2008).
24. A. B. Molofsky, J. C. Nussbaum, H. E. Liang, S. J. van Dyken, L. E. Cheng, A. Mohapatra, A. Chawla, R. M. Locksley, Innate lymphoid type 2 cells sustain visceral adipose tissue eosinophils and alternatively activated macrophages. *J. Exp. Med.* **210**, 535–549 (2013).
25. M. Wills-Karp, R. Rani, K. Dienger, I. Lewkowich, J. G. Fox, C. Perkins, L. Lewis, F. D. Finkelman, D. E. Smith, P. J. Bryce, E. A. Kurt-Jones, T. C. Wang, U. Sivaprasad, G. K. Hershey, D. R. Herbert, Trefoil factor 2 rapidly induces interleukin 33 to promote type 2 immunity during allergic asthma and hookworm infection. *J. Exp. Med.* **209**, 607–622 (2012).
26. B. Griesenauer, S. Paczesny, The ST2/IL-33 axis in immune cells during inflammatory diseases. *Front. Immunol.* **8**, 475 (2017).
27. A. M. Miller, D. L. Asquith, A. J. Hueber, L. A. Anderson, W. M. Holmes, A. N. McKenzie, D. Xu, N. Sattar, I. B. McInnes, F. Y. Liew, Interleukin-33 induces protective effects in adipose tissue inflammation during obesity in mice. *Circ. Res.* **107**, 650–658 (2010).
28. T. Mahlakõiv, A. L. Flamar, L. K. Johnston, S. Moriyama, G. G. Putzel, P. J. Bryce, D. Artis, Stromal cells maintain immune cell homeostasis in adipose tissue via production of interleukin-33. *Sci. Immunol.* **4**, eaax0416 (2019).
29. A. Vasanthakumar, K. Moro, A. Xin, Y. Liao, R. Gloury, S. Kawamoto, S. Fagarasan, L. A. Mielke, S. Afshar-Sterle, S. L. Masters, S. Nakae, H. Saito, J. M. Wentworth, P. Li, W. Liao, W. J. Leonard, G. K. Smyth, W. Shi, S. L. Nutt, S. Koyasu, A. Kallies, The transcriptional regulators IRF4, BATF and IL-33 orchestrate development and maintenance of adipose tissue-resident regulatory T cells. *Nat. Immunol.* **16**, 276–285 (2015).
30. J. M. Han, D. Wu, H. C. Denroche, Y. Yao, C. B. Verchere, M. K. Levings, IL-33 reverses an obesity-induced deficit in visceral adipose tissue $ST2^+$ T regulatory cells and ameliorates adipose tissue inflammation and insulin resistance. *J. Immunol.* **194**, 4777–4783 (2015).
31. Z. Chen, G. X. Wang, S. L. Ma, D. Y. Jung, H. Ha, T. Altamimi, X. Y. Zhao, L. Guo, P. Zhang, C. R. Hu, J. X. Cheng, G. D. Lopaschuk, J. K. Kim, J. D. Lin, Nrg4 promotes fuel oxidation and a healthy adipokine profile to ameliorate diet-induced metabolic disorders. *Mol. Metab.* **6**, 863–872 (2017).
32. J. I. Odegaard, M. W. Lee, Y. Sogawa, A. M. Bertholet, R. M. Locksley, D. E. Weinberg, Y. Kirichok, R. C. Deo, A. Chawla, Perinatal licensing of thermogenesis by IL-33 and ST2. *Cell* **166**, 841–854 (2016).
33. M. W. Lee, J. I. Odegaard, L. Mukundan, Y. Qiu, A. B. Molofsky, J. C. Nussbaum, K. Yun, R. M. Locksley, A. Chawla, Activated type 2 innate lymphoid cells regulate beige fat biogenesis. *Cell* **160**, 74–87 (2015).
34. S. Li, L. Mi, L. Yu, Q. Yu, T. Liu, G. X. Wang, X. Y. Zhao, J. Wu, J. D. Lin, Zbtb7b engages the long noncoding RNA Blnc1 to drive brown and beige fat development and thermogenesis. *Proc. Natl. Acad. Sci. U.S.A.* **114**, E7111–E7120 (2017).
35. X. Y. Zhao, S. Li, J. L. DelProposto, T. Liu, L. Mi, C. Porsche, X. Peng, C. N. Lumeng, J. D. Lin, The long noncoding RNA Blnc1 orchestrates homeostatic adipose tissue remodeling to preserve metabolic health. *Mol. Metab.* **14**, 60–70 (2018).
36. P. E. Collins, I. Mitxitorena, R. J. Carmody, The ubiquitination of NF-κB subunits in the control of transcription. *Cells* **5**, E23 (2016).
37. M. Davis, A. Hatzubai, J. S. Andersen, E. Ben-Shushan, G. Z. Fisher, A. Yaron, A. Bauskin, F. Mercurio, M. Mann, Y. Ben-Neriah, Pseudosubstrate regulation of the $SCF^{\beta\text{-}TrCP}$ ubiquitin ligase by hnRNP-U. *Genes Dev.* **16**, 439–451 (2002).
38. V. Francisco, J. Pino, V. Campos-Cabaleiro, C. Ruiz-Fernández, A. Mera, M. A. Gonzalez-Gay, R. Gómez, O. Gualillo, Obesity, fat mass and immune system: Role for leptin. *Front. Physiol.* **9**, 640 (2018).
39. Y. Luo, M. Liu, Adiponectin: A versatile player of innate immunity. *J. Mol. Cell Biol.* **8**, 120–128 (2016).
40. G. X. Wang, X. Y. Zhao, Z. X. Meng, M. Kern, A. Dietrich, Z. Chen, Z. Cozacov, D. Zhou, A. L. Okunade, X. Su, S. Li, M. Blüher, J. D. Lin, The brown fat-enriched secreted factor Nrg4 preserves metabolic homeostasis through attenuation of hepatic lipogenesis. *Nat. Med.* **20**, 1436–1443 (2014).
41. J. R. Brestoff, B. S. Kim, S. A. Saenz, R. R. Stine, L. A. Monticelli, G. F. Sonnenberg, J. J. Thome, D. L. Farber, K. Lutfy, P. Seale, D. Artis, Group 2 innate lymphoid cells promote beiging of white adipose tissue and limit obesity. *Nature* **519**, 242–246 (2015).
42. Y. H. Lin, R. C. Zhang, L. B. Hou, K. J. Wang, Z. N. Ye, T. Huang, J. Zhang, X. Chen, J. S. Kang, Distribution and clinical association of plasma soluble ST2 during the development of type 2 diabetes. *Diabetes Res. Clin. Pract.* **118**, 140–145 (2016).
43. L. Wang, K. F. Wildt, E. Castro, Y. Xiong, L. Feigenbaum, L. Tessarollo, R. Bosselut, The zinc finger transcription factor Zbtb7b represses CD8-lineage gene expression in peripheral $CD4^+$ T cells. *Immunity* **29**, 876–887 (2008).
44. D. Ma, M. M. Molusky, J. Song, C. R. Hu, F. Fang, C. Rui, A. V. Mathew, S. Pennathur, F. Liu, J. X. Cheng, J. L. Guan, J. D. Lin, Autophagy deficiency by hepatic FIP200 deletion uncouples steatosis from liver injury in NAFLD. *Mol. Endocrinol.* **27**, 1643–1654 (2013).
45. S. Li, C. Liu, N. Li, T. Hao, T. Han, D. E. Hill, M. Vidal, J. D. Lin, Genome-wide coactivation analysis of PGC-1α identifies BAF60a as a regulator of hepatic lipid metabolism. *Cell Metab.* **8**, 105–117 (2008).
46. K. W. Cho, D. L. Morris, C. N. Lumeng, Flow cytometry analyses of adipose tissue macrophages. *Methods Enzymol.* **537**, 297–314 (2014).
47. K. W. Cho, B. F. Zamarron, L. A. Muir, K. Singer, C. E. Porsche, J. B. DelProposto, L. Geletka, K. A. Meyer, R. W. O'Rourke, C. N. Lumeng, Adipose tissue dendritic cells are independent contributors to obesity-induced inflammation and insulin resistance. *J. Immunol.* **197**, 3650–3661 (2016).

Acknowledgments: We thank R. Bosselut from NCI for sharing the Zbtb7b flox mouse strain. **Funding:** This work was supported in part by NIH (DK102456 and DK118731 to J.D.L.) and the Michigan Diabetes Research Center and the Michigan Nutrition and Obesity Research Center (P30-DK020572 and P30-DK089503). X.-Y.Z. was supported by an NIH Pathway to Independence Award (DK106664). Y.J. was supported by an AHA Scientist Development Grant (17SDG33670192). **Author contributions:** J.D.L. and X.-Y.Z. conceived the project and designed research. X.-Y.Z., Z.C., S.L., Y.J., and X.P. performed the experiments and analyzed data. L.Z., Y.J., and L.Q. performed flow cytometry analysis. J.D.L. and X.-Y.Z. wrote the manuscript. **Competing interests:** The authors declare that they have no competing interests. **Data materials and availability:** All data needed to evaluate the conclusions in the paper are present in the paper and/or the Supplementary Materials. Additional data related to this paper may be requested from the authors.

Submitted 4 July 2019
Accepted 2 March 2020
Published 13 May 2020
10.1126/sciadv.aay6191

Citation: X.-Y. Zhao, L. Zhou, Z. Chen, Y. Ji, X. Peng, L. Qi, S. Li, J. D. Lin, The obesity-induced adipokine sST2 exacerbates adipose T_{reg} and ILC2 depletion and promotes insulin resistance. *Sci. Adv.* **6**, eaay6191 (2020).